An auxin-mediated ultradian rhythm promotes root regeneration in Arabidopsis

Quy Vu
Institute for Basic Science
Kitae Song
Institute for Basic Science
Sung-Jin Park
Institute for Basic Science
Lin Xu
CAS Center for Excellence in Molecular Plant Sciences, Institute of Plant Physiology and Ecology, Chinese Academy of Sciences https://orcid.org/0000-0003-4718-1286
Hong Gil Nam
Center for Plant Aging Research, Institute for Basic Science (IBS) https://orcid.org/0000-0003-2296-5447
Sunghyun Hong (shhong@ibs.re.kr)
Institute for Basic Science

Article

Keywords: ultradian rhythm, Arabidopsis, root regeneration,

Posted Date: June 25th, 2021

DOI: https://doi.org/10.21203/rs.3.rs-604908/v1

Abstract

Ultradian rhythms have been proved to be critical for diverse biological processes. However, comprehensive understanding of the short-period rhythms remains limited. Here, we discover that leaf excision triggers a gene expression rhythm with ~ 3-h periodicity, named as the excision ultradian rhythm (UR), which is regulated by the plant hormone auxin. Transcriptome analysis found more than 4,000 excision UR genes which are diverse in terms of biological function. Promoter–luciferase analyses showed that the spatiotemporal patterns of the excision UR were positively associated with *de novo* root regeneration (DNRR), a post-embryonic developmental process. Genetic studies showed that EXCISION ULTRADIAN RHYTHM 1 (EUR1), which encodes ENHANCER OF ABSCISIC ACID CO-RECEPTOR1 (EAR1), an abscisic acid signaling regulator, was required to generate the excision ultradian rhythm and promote root regeneration. Moreover, the *ear1* mutant exhibited the absence of auxin-induced excision UR generation and partial failure to rescue DNRR. These results demonstrate that leaf excision activates EAR1-mediated excision UR and reprograms the expression of a large set of genes involved in DNRR.

Main

Biological rhythms are ubiquitous periodic cycles that impact the physiology, behavior and transcriptome of living organisms and play critical roles in their ecological fitness [1,2]. In addition to well-known circadian (~ 24-h) rhythms, ultradian (< 24-h) rhythms, despite a much smaller number of studies [3], have been reported to be critical for diverse biological processes in both animals and plants such as development, cell fate decision and metabolism [4-7]. In plants, the most notable ultradian rhythm (UR) is the cytosolic calcium oscillations in guard cells, which is required for stomatal closure [8-10]. In *Arabidopsis thaliana*, periodic root branching is accompanied by a ~6-h gene expression rhythm and disruption of this rhythmic gene expression impairs root formation [5]. Ultradian rhythms display an enormous diversity in periodic phenomena with various frequencies and characteristics [11,12]; therefore, origin and biological significance of ultradian rhythms remain opened questions and many biological processes which may be associated with ultradian rhythms have not been identified yet. Here, we serendipitously discovered a ultradian gene expression rhythm in excised *Arabidopsis* leaves and investigated the physiological relevance and the genetic mechanism underlying the occurrence of this rhythm.

The ability to regenerate organs and tissues, particularly after predator attack or mechanical wounding, is a critical survival mechanism that allows organisms to replace or augment lost or damaged organs and tissues. Recent studies revealed extensive molecular regulatory mechanisms underlying regeneration in animals and plants, and highlighted their potential application in regenerative medicine and agriculture [13,14]. Plants possess a unique and remarkable regeneration capability. Plant regeneration not only replaces lost tissue and organs, but can also lead to the genesis of new organs and even entire organisms [15]. This unique capability, given their sessile lifestyle, allows plants to optimize survival and propagation under hostile ecological situations [16]. Genesis of new organs from organ explants or *de novo* organogenesis allows plants to develop new organs such as shoots or roots from excised parts of

plants, and this is frequently observed in nature [17]. Excised *Arabidopsis* leaves, which can regenerate adventitious roots (ARs) at the excision site on a hormone-free medium, are frequently used as a model system to imitate natural conditions and investigate the molecular mechanisms underlying *de novo* root regeneration (DNRR) [18]. DNRR is a highly complex process that involves time-evolving regulatory networks with a series of cell fate transition, division and differentiation steps which require reprogramming of large set of gene expression [19,20]. Despite recent extensive studies, the regulatory mechanisms of gene expressions underlying the DNRR process are not fully understood.

The results presented here show a new regulatory layer that a UR triggered by leaf excision promotes DNRR by resetting gene expression patterns, thereby assisting the cells at the excision sites to reorient from their predetermined differentiated cellular states toward new fates.

Results

Leaf excision evokes an auxin-mediated UR

We previously used the firefly *luciferase* (*LUC*) reporter gene [21,22] to track the promoter activities of circadian clock-regulated genes, including *ORE1*, in transgenic *Arabidopsis*. The 3rd or 4th rosette leaves were excised from 21-day-old plants grown under long-day conditions (16 h light/8 h dark), and LUC activity was monitored at 30 min intervals using a CCD camera under continuous white light at 22°C. (Fig. 1a). Transgenic *ORE1::LUC* plants showed short period rhythms (Fig. 1b). We used wavelet analysis, which is suitable for time-frequency data [23], to determine whether periodicity resulted from an endogenous biological rhythm. As the *ORE1* promoter exhibited a circadian rhythm (CR) as well as UR, we separated the circadian component by reconstructing the smoothed circadian signal from the original oscillating pattern. Consequently, the wavelet spectrum exhibited a ~24 h period CR (Fig. 1c). Subtraction of the CR wavelet from the original oscillating pattern revealed an additional UR with a ~3 h period (Fig. 1d). *ORE1*, *CCA1*, *PRR7* and *CAB2* promoter activities in excised leaves showed similar periods of ~3 h, with various wavelet powers (Fig. 1e and Supplementary Fig. 1). When a threshold of 1.0 was established to discriminate the UR from noise (Fig. 1e, red line), *ORE1* promoter activity showed a significant wavelet power. We further characterized this ~ 3 h rhythm using *ORE1* promoter activity.

We used wavelet analysis of *ORE1* promoter activity to determine whether the UR was present in intact leaves and other excised organs. Attached leaves did not exhibit a UR in *ORE1* promoter activity (Supplementary Fig. 2a-c,n). Next, we examined *ORE1* promoter activity in 7-day-old whole seedlings and in excised shoot apices, cotyledons, hypocotyls and roots (Supplementary Fig. 2d). The UR was detected in excised cotyledons but not in the other samples (Supplementary Fig. 2e-i,n). We also tested organs excised from bolted plants (Supplementary Fig. 2j). The UR was present in excised cauline leaves but not in excised flowers or stems (Supplementary Fig. 2k-n). Thus, the *ORE1* UR is leaf specific and is evoked upon its excision. The ~3 h period UR was therefore named the ‘excision UR’.

To gain insight into the physiological function of the excision UR, we examined its temporal and spatial expression patterns in excised leaves. A significant excision UR wavelet power was observed from ~19 h after excision and maintained until ~ 60 h before dampening over time (Fig. 1f). The excision UR thus functioned as a transient response to excision. The highest level of *ORE1* promoter activity with robust oscillations was observed in the petiole region close to the excision site (Fig. 1g). By contrast, *ORE1* promoter activity persisted across the whole area of an attached leaf (Supplementary Movie 1). The localized and transient nature of the UR proximate to the excision site supported the conclusion it was a response to leaf excision.

Excised *Arabidopsis* leaves undergo a drastic developmental shift toward *DNRR* at the excision site. By ~12 h after excision, auxin is produced in converter cells and transported to the vasculature near the wound site, where it is involved in further DNRR processes [19,20,24,25]. These studies suggested the excision UR might be related to the production of auxin as an excision response. To test this, we monitored auxin responses *in vivo* and in real time using *DR5::LUC* transgenic plants [5]. *DR5::LUC* expression exhibited an excision UR with a significant wavelet power (Fig. 1h,i). Activity was enriched in the petiole region (Fig. 1j). Furthermore, the average wavelet power of the *ORE1* promoter excision UR was reduced by yucasin, an auxin biosynthesis inhibitor [26], and rescued by exogenous auxin (Fig. 1k), indicating that auxin positively regulated the excision UR in excised leaves. However, treatment of young, excised leaves with exogenous auxin did not significantly affect the UR wavelet power (Fig. 1k), suggesting that endogenous auxin levels were sufficient for UR generation in young leaves. Leaf excision thus generated an auxin-regulated excision UR.

Function and expression of a large set of excision UR genes

Time-lapse transcriptome analysis was used to examine the physiological roles of the excision UR further. We used MetaCycle analysis, an established method for evaluating periodicity in time-series data [27], to identify genes involved in the excision UR at the transcriptional level. Expression of 4,073 genes oscillated with period lengths between 2.9 and 4.3 h (Fig. 2a and Supplementary Table 1), indicating that a relatively large set of genes displayed a ultradian oscillation in response to leaf excision. Gene Ontology (GO) analysis revealed these genes encompassed a broad range of biological processes. The GO terms ‘responses to stimuli’, ‘metabolic process’ and ‘developmental process’ were enriched (Fig. 2b and Supplementary Table 1). A further enrichment analysis using the Kyoto Encyclopedia of Genes and Genomes (KEGG) database (Fig. 2c) found ‘plant hormone signal transduction’ (KEGG:04075) was the most strongly enriched pathway, as 61 excision UR genes were annotated in this pathway (Supplementary Table 2). The excision UR was therefore involved in resetting various hormonal signaling pathways. Several metabolic pathways were also enriched among the excision UR genes. The excision UR thus predominantly involved genes acting in hormone signal transduction pathways and multiple metabolic processes.

DNRR at the leaf excision site involves a complex array of regulatory genes. Auxin plays an essential role in this process [18-20,24,25]: of 35 DNRR-associated genes identified previously, ten, of which seven were

auxin-related, showed the UR expression pattern (Supplementary Table 3). The excision UR thus regulated the expression of genes involved in auxin-related DNRR. Auxin regulates a root clock, which produces oscillations in gene expression with a ~6 h period for prebranch site production [5]. We compared the genes showing ~3 h period UR with microarray data from the root clock to determine whether these different URs shared common molecular components. Although the two datasets showed little overlap (< 7%), *YUCCA 9* (*YUC9*) and *AUXIN RESPONSIVE FACTOR 7* (*ARF7*) were common to both (Supplementary Fig. 3). Both are auxin-related genes involved in DNRR, suggesting that, although the two URs controlled distinct sets of genes, they shared part of the auxin-mediated regulatory pathways.

The effect of the excision UR on auxin-related genes was confirmed using promoter-reporter assays. LUC activity in transgenic plants expressing *PIN-FORMED 3* (*PIN3*)*::LUC*, *ARF7::LUC* or *AUXIN SIGNALING F-BOX 2* (*AFB2*)*::LUC* showed robust excision UR (Fig. 2d-g). Reciprocal regulation between auxin and the excision UR led us to test whether the auxin signaling pathway was involved in generating the UR. We screened the oscillating auxin-related genes *ARFs* (*ARF4*, *7*, *8* and *10*), *PIN3*, *AFB2* and *TRANSPORT INHIBITOR RESPONSE 1* (*TIR1*) by examining patterns of *ORE1::LUC* expression in loss-of-function mutants, as well as in a gain-of-function mutant of *SHORT HYPOCOTYL 2* (*SHY2*). Excised leaves from all mutants showed a robust excision UR (Supplementary Fig. 4), suggesting it was either generated upstream of auxin signaling or was genetically separate from the auxin signaling pathway.

Positive correlation between excision UR and DNRR

As both the excision UR and DNRR were induced by leaf excision and controlled by auxin, we assessed the relationship between robustness of the excision UR and efficiency of DNRR in excised leaves under various conditions. DNRR is highly sensitive to the age of an excised leaf [18,28], with aged leaves exhibiting a marked reduction in DNRR capacity. The excision UR and DNRR efficiency were examined in leaves excised from plants of different ages. The average wavelet powers of the excision UR were robust in the 4th leaf from 17- or 21-day-old plants, but gradually decreased with leaf age; the excision UR was not detectable in leaves from 28-day-old plants (Fig. 3a). The efficiency of DNRR was positively correlated with the trend in excision UR (Fig. 3b,c). Thus both the excision UR and DNRR were highly sensitive to leaf age, and occurrences of the two events were correlated.

DNRR is sensitive to light conditions, as excised leaves form roots under light conditions but not in the dark without sucrose [18]. We therefore examined the effect of varying light intensity on excision UR robustness and DNRR efficiency. The average wavelet powers of the excision UR were highest under photosynthetically active radiation (PAR) of 20 mmol m^{-2} s^{-1}, and were reduced in the dark and under lower or higher light intensities (Fig. 3d). Similarly, DNRR was most efficient under PAR of 20 mmol m^{-2} s^{-1} (Fig. 3e). Excised leaves did not produce any roots under darkness due to dark-induced senescence, a rapid ageing process (Fig. 3f). Leaves exposed to lower and higher light intensities remained green for 12 days after excision but showed reduced DNRR efficiency (Fig. 3e,f). Excision UR robustness was therefore positively correlated with DNRR efficiency under various light intensities.

EAR1, an abscisic acid (ABA) signaling component, positively regulates the excision UR to optimize DNRR

A forward genetic screen was performed to search for genetic factors involved in excision UR generation and/or function. Transgenic *ORE1::LUC* seeds were mutagenized with ethyl methane sulfonate (EMS). Leaves excised from individual M_2 plants were screened for the absence of the excision UR. Four homozygous lines (*M21*, *23*, *38* and *83*) were identified after screening ~16,000 M_2 plants (Fig. 4a-e; Supplementary Fig. 5a, b). Genetic analyses revealed that all four candidates were recessive mutants. *M21*, *M23* and *M83* belonged to the same complementation group, whereas *M38* formed a second distinct complementation group (Supplementary Fig. 5c). The mutations were named *EXCISION ULTRADIAN RHYTHM* (*EUR*), and the first and second complementation groups were named *EUR1* and *EUR2*, respectively. All four mutants exhibited delayed initiation of ARs relative to wild type (Fig. 4f and Supplementary Fig. 5d). These results supported a causative association of UR with DNRR, as the four mutants belonged to two independent complementation groups, and yet controlled the excision UR and DNRR simultaneously.

The presence of three *eur1* mutant alleles in one complementation group facilitated molecular analysis by whole-genome sequencing (WGS). The WGS data of *ORE1::LUC* (parental line) were compared with that of a pool of F_2 homozygous mutant progeny, which showed no excision UR, obtained by backcrossing *M21* or *M83* with *ORE1::LUC*. Only one gene, *ENHANCER OF ABSCISIC ACID (ABA) CO-RECEPTOR1* (*EAR1*), harboured common intragenic single nucleotide polymorphisms (SNPs) in both the *M21* and *M83* mutants (Supplementary Fig. 5e). The WGS results were validated by sequencing the *EAR1* coding sequence in *M21*, *M83* and *M23* (Supplementary Fig. 5f). In *M21* and *M23*, tryptophan residues at amino acid positions 112 and 52 were changed to nonsense codons, whereas glycine-157 was changed to glutamate in *M83* (Fig. 4g). The mutant alleles in *M21*, *M23* and *M83* were named *eur1-11*, *eur1-12* and *eur1-13*, respectively. To confirm that *EAR1* was the gene responsible for the excision UR, complementation lines (*COM-9*, *COM-24*) were generated by expressing an *EAR1-GFP* fusion construct under the control of its cognate promoter (*EAR1::EAR1-GFP*) in the *eur1-11* mutant background. The expression of *EAR1::EAR1-GFP* rescued both the impaired excision UR and reduced DNRR efficiency phenotypes of *eur1-11* (Supplementary Fig. 6). These results indicated that *EAR1* corresponded with the *eur1* mutations and was a positive regulator of excision UR in excised *Arabidopsis* leaves.

EAR1 is a negative regulator of ABA signaling, and the core $EAR1^{141-287}$ fragment is sufficient for EAR1 function in ABA responses [29]. We tested whether the core fragment of EAR1/EUR1 generated the UR in a similar manner by using an insertion line of *EAR1* (SALK_108025, *eur1-14*), in which the T-DNA is inserted at position 1,338 of *AT5G22090* (Fig. 4g), keeping the core fragment intact. Unlike the other *eur1* mutant alleles, ABA responses, inhibition of germination and root growth in *eur1-14* resembled those of wild-type plants (Fig. 4h,i), confirming previous reports [29]. Notably, however, both expression of the excision UR and DNRR efficiency were impaired in *eur1-14* leaves (Fig. 4j,k), suggesting that EAR1/EUR1-mediated excision UR generation and AR formation are separate from canonical ABA signaling.

Auxin-induced generation of the excision UR via *EAR1/EUR1 promotes DNRR*

As the EAR1/EUR1 controlled both the excision UR and DNRR, we investigated the link between these two phenomena. We performed time-course RNA-seq analysis of the petiole regions of wild-type and *eur1-11* mutant leaves collected at 0, 24, 48, 72 and 96 h after excision. This revealed that 9,754 genes were differentially expressed between wild type and *eur1-11*. These differentially expressed genes (DEGs) were categorized into 12 clusters according to the similarity between their expression profiles (Supplementary Fig. 7 and Supplementary Table 4). Interestingly, the expression profiles of genes in cluster 2, which contained *EAR1/EUR1*, resembled the pattern of excision UR wavelet power (Fig. 5a). To gain further insight into the role of EAR1/EUR1 in DNRR, we performed GO and KEGG enrichment analyses of the 325 genes belonging to cluster 2. These genes were strongly enriched in GO/KEGG terms related to auxin and development (Fig. 5b), suggesting that EAR1/EUR1 promoted DNRR *via* an auxin-mediated molecular mechanism. Indeed, the DNRR-associated genes found in cluster 2 included key genes required for auxin biosynthesis and transport, and for auxin-mediated cell fate transition, such as *YUC8*, *YUC9*, *PIN2* and *WUSCHEL-RELATED HOMEOBOX 11* (*WOX11*) [19,24] (Fig. 5c). The absence of EAR1/EUR1 altered auxin signaling in the petiole region upon excision, which may have changed the expression of genes involved in cell fate determination and resulted in reduced DNRR efficiency.

DNRR occurs at the site of excision from the petiole. Excision UR expression was the strongest at the petiole, which correlated positively with DNRR. We therefore examined the spatial and temporal regulation of EAR1/EUR1 in *EAR1::EAR1-GFP* plants. The fluorescence signal was absent in the petiole region at 0 days after excision (DAE), but was visible from 1 DAE and most abundant at 2 DAE (Fig. 5d), indicating that the changes in EAR1/EUR1 levels coincided with expression of the excision UR.

Exogenous application of auxin rescues DNRR in aged leaves [18]. As the excision UR was also regulated by auxin (Fig. 1f) and reduced in aged leaves (Fig. 3a), we hypothesized that auxin might induce the excision UR through EAR1/EUR1 and rescue DNRR efficiency in aged leaves. To test this, we applied 10 μM IAA to 4th rosette leaves excised from aged (24-day-old) wild-type and *eur1-11* mutant plants, and measured robustness of the excision UR and DNRR efficiency. Exogenous auxin treatment rescued the excision UR wavelet power in aged wild-type leaves but not in aged *eur1-11* leaves (Fig. 5e), indicating that EAR1/EUR1 was required for auxin-induced excision UR generation. The DNRR efficiency of aged wild-type leaves was also fully rescued by auxin; however, aged *eur1-11* mutant leaves showed lower DNRR efficiency than their wild-type counterparts (Fig. 5f), indicating that the EAR1/EUR1-mediated excision UR was necessary to promote DNRR, although auxin could induce DNRR independently. All these results suggest that leaf excision triggers an endogenous oscillation in gene expression that promotes root regeneration, and this process is regulated by reciprocal interactions between auxin and EAR1/EUR1 (Fig. 5g).

Discussion

Here, we show that, in *Arabidopsis*, leaf excision activates EAR1/EUR1, which acts *via* auxin to generate a transient excision UR that promotes AR formation. Like other ultradian rhythms in gene expression, such as the root branching rhythm in *Arabidopsis* [5], segmentation and somitogenesis in *Drosophila* [30], this

excision UR is involved in a developmental process, DNRR. In addition, like root clock [5] and segmentation clock [31], there might be a ultradian clock to regulate this excision UR, in which *EUR1* and *EUR2* play a role as core clock genes. However, the excision UR is not associated with a spatially periodic modular developmental pattern. Instead, it is evoked *de novo* at the petiole region of excised leaves and is observed transiently after excision. Thus, the latent and transient excision UR has a unique oscillatory feature. DNRR is a highly complex process that involves regulatory networks that change over time and show three distinct phases [19,20]. The time-frame of the excision UR overlapped with phase II (auxin accumulation) and phase III (cell fate transition) (Fig. 1f and Supplementary Table 3). Therefore, cells undergo fate transition when the EUR is robust. This timing is indicative of the role of the latent and transient excision UR in biological processes. In addition, expression of cell fate transition genes was altered in *eur1-11* mutants (Fig. 5c). Rhythmic gene expression at the excision site may serve as a means of resetting and reprogramming gene expression to facilitate cell fate transition. This would resemble the situation in lateral root development, in which oscillatory behaviour of some genes is associated with cell fate transition in response to lateral root initiation [5,32]. URs with frequent information may temporally govern gene expression to precisely control cell fate transitions during development in plants.

Robustness of the excision UR was affected by developmental stage of leaves and environmental signals such as light intensity, which also influence DNRR efficiency (Fig. 3). As plants age, gradually increased transcription factors such as *SQUAMOSA PROMOTER BINDING PROTEIN-LIKE* (*SPL*) *2/10/11* and *ETHYLENE INSENSITIVE 3* (*EIN3*) repress root regeneration by inhibiting auxin biosynthesis and expression of cell fate transition genes, respectively [33,34]. Auxin, a major hormone in DNRR, was required for generation of the excision UR (Fig. 1k) and also rescued the excision UR in aged leaves (Fig. 5e). This indicates that the excision UR as well as DNRR are positively regulated by auxin which level is gradually decreased along with the age of leaves. Proper light intensity was required for optimal generation of the excision UR (Fig. 3d). This may be caused by an imbalance in carbohydrate concentration, which is otherwise required for optimal DNRR (Fig. 3e,f). Previous study showed that, in excised leaves, sucrose is required in the dark to regenerate ARs, but somewhat represses root regeneration in the light [18], suggesting that an appropriate amount of carbohydrate is necessary for optimal root regeneration as an energy source. Lower robustness of the excision UR in the dark (Fig. 3d) might also be caused by depletion of energy which can be made by photosynthesis in the light. As only leaves can make enough energy source via photosynthesis in the light, leaf-specific occurrence of the excision UR (Supplementary Fig. 2) supports this explanation.

Leaf excision and subsequent DNRR processes are largely integrated by the interplay of several hormones, including early signaling by the wound hormone jasmonic acid followed by various auxin, cytokinin and ethylene [35]. This is consistent with the KEGG pathway analysis of the excision UR transcriptome (Fig. 2c) as the excision UR is associated with DNRR. However, the role of ABA signaling components in DNRR has been rarely discussed to date. One of the regulators of the excision UR identified from genetic screening was EAR1/EUR1, previously known as a negative regulator of ABA signaling [29]. Interestingly, EAR1/EUR1 is involved in canonical ABA responses, but the excision UR

mediated by EAR1/EUR1 may be generated by a different molecular mechanism (Fig. 4h-k), which is positively regulated by auxin. EAR1/EUR1 controls genes from the auxin pathway, including auxin biosynthesis genes, resulting in a reciprocal positive feedback loop between auxin and EAR1/EUR1 (Fig. 5g). ABA is generally considered as a negative regulator of AR formation [35]. Therefore, although EAR1/EUR1-mediated excision UR generation and root regeneration was decoupled from canonical ABA responses, EAR1/EUR1 may also regulate ABA signaling during DNRR by activation of the ABA co-receptor phosphatases that negatively regulate ABA signaling, and to evoke the EUR at the excision site. Consistent with these, the expression of EAR1/EUR1 is activated at the excision site of petiole, as would be expected for the petiole excision site to be competent for cell fate transition and division. Further studies to identify more components, such as other *eur* mutants or factors interacting with EAR1/EUR1, will improve our understanding of the regulatory mechanisms underlying the excision UR and DNRR.

Methods

Plant materials and growth conditions

Arabidopsis thaliana ecotype Columbia (Col-0) was used as wild-type control. The transgenic *CCA1::LUC* [36], *CAB2::LUC* [37], *ORE1::LUC* [21], *DR5::LUC* [5] and *ARF7::LUC* [5] lines, *shy2-1D* [38] *and tir1-1* [39] have previously been described. *PRR7::LUC* was kindly donated by Xie and McClung. To generate the *PIN3::LUC* and *AFB2:LUC,* 2,031 bp of *PIN3* and 2,078 bp of *AFB2* promoter regions were cloned into the pZPXomegaLUC vector [40] to fuse with the firefly luciferase gene and they were introduced into Col-0 plants by Agrobacterium tumefaciens-mediated transformation. The transgenic *ORE1::LUC* in *arf4* (SALK_070506C)*, arf7* (CS_873146)*, arf8* (CS_870172)*, arf10* (SALK_087247C)*, pin3* (SALK_113248C)*, afb2* (CS_819008), *tir1-1* and *eur1-14* (SALK_108025C), were generated by Agrobacterium tumefaciens-mediated transformation and *shy2-1D* [38] mutant expressing *ORE1::LUC* were generated by genetic crossing. For complementation of *eur1-11* mutant, *EAR1::EAR1-GFP* was constructed by fusing a combination of full length genomic DNA fragment without stop codon and 2,092 bp of promoter fragment of *EAR1* in front of Green Fluoresent Protein (GFP) in the gCogn-eGFP-N-1300 (Cambia, Canberra, Australia). See Supplementary Table 5 for primer details. *Arabidopsis thaliana* plants were grown in an environmentally controlled growth room (Korea Instruments, Korea) at 22^{o}C under 16 h light/8 h dark conditions with ~100 μmol $m^{-2}s^{-1}$ white light. For confocal microscopic assay, Col/*EAR1::EAR1-GFP* seeds were surface-sterilized with 1% sodium hypochlorite for 10 min and rinsed 4 times with sterilized distilled water. After 3 days in cold condition, sterilized seeds were planted on half strength B5 medium (Duchefa, The Netherlands) containing 0.8% agar (type M; Sigma) with 1% sucrose and grown in the same condition.

Luminescence assay

Transgenic plants expressing luciferase under control of various gene promoters were used in this assay. Whole seedlings, or indicated samples were excised from transgenic plants and transferred to 48- or 24-well microplates containing 5.7 pH of 3 mM MES (2-(N-morpholino) ethanesulfonic acid, Amresco, USA)

solution with 500 μM luciferin (SYNCHEM, Felsberg/Altenburg, Germany). Those plates were put in luminescence chambers under continuous light (~20 μmol m^{-2} s^{-1}) condition at 22°C. Luminescence images were acquired every 30 min with 5-min exposure times for at least 3 days and images were analyzed with the MetaView system (Molecular Devices, USA).

Wavelet analysis for detecting rhythms

The luminescence intensities were quantified by continuous wavelet transformation techniques, which are implemented into Wavelet Comp package in R [41] for detecting circadian rhythm (CR) and ultradian rhythm (UR). The rhythms were detected by periodic parameters of 2 to 6 hours for UR and 16 to 32 hours for CR.

De novo root regeneration assay

For root regeneration assay, the 4th rosette leaves were excised from indicated ages of plants and placed on half strength B5 medium (Duchefa, The Netherlands) (pH 5.7) containing 0.8% agar without sucrose. To prevent fungal contaminations, we added plant preservative mixture (PPM) (Plant cell technology, Washington, USA) with ratio 1:3,000. The plates were cultured under continuous light conditions with ~20 μmol $m^{-2}s^{-1}$ white light at 22°C. The number of adventitious roots from leaf explants was determined by counting the regenerated root tips in the petiole regions during the indicated day. The rooting rate was calculated as the ratio of root tip regeneration to total cultured leaf explants on the indicated day. The rooting images were taken using a SMZ1500 stereomicroscope (Nikon, Japan), with 0.75× objective.

Sampling to identify UR oscillating genes

The 4th rosette leaves from soil-grown 21 day-old plants were excised at their petiole by forceps and floated in plates containing 3 mM MES solution (pH 5.7). Plates were incubated under dark and 16°C for 24 hours and then transferred to ~20 μmol $m^{-2}s^{-1}$ continuous white light condition at 22°C. Leaves were collected at 16 different time points between 19 and 27 hours after pre-treatment. Total cellular mRNA was extracted from WelPrep (Welgene, Daegu, Korea). Contaminating DNA was removed by digestion with DNase I (DNA-*free*™ Kit DNase Treatment and Removal, Invitrogen, Thermo Fisher Scientific), then RNA quality was assessed on an Agilent BioAnalyzer 2100. RNA integrity numbers (RINs) for the samples were calculated and found the average RIN to be 7.5 with which many mRNA-sequencing experiments have been performed.

Sampling for RNA-seq to identify DEGs between wild-type and *eur1-11*

The 4th rosette leaves from soil-grown 21 day-old plants of Col/*ORE1::LUC* as wild-type and *eur1-11* mutant were excised at their petiole by forceps and floated in plates containing 3mM MES solution (pH 5.7). Plates were incubated under ~20 μmol $m^{-2}s^{-1}$ continuous white light conditions at 22°C. Petiole regions of excised leaves were collected at 0, 24, 48, 72 and 96h since detachment. Total mRNA was extracted from leaves using WelPrep (Welgene, Daegu, Korea). Contaminating DNA was removed by

digestion with DNase I (DNA-*free*™ Kit DNase Treatment and Removal, Invitrogen, Thermo Fisher Scientific), then RNA quality was assessed on an Agilent BioAnalyzer 2100.

RNA-seq and functional prediction

Library construction and sequencing were performed using Illumina Hiseq 2500 platform for detecting oscillation genes and using Illumina NovaSeq 6000 platform for eur*1-11*. Raw reads were checked quality and trimmed using FastQC [42], and the trimmed reads were mapped to the Arabidopsis thaliana genome (TAIR10) using STAR [43]. After alignment, the gene-level raw count data files were generated using HTSeq [44] and normalized using edgeR's TMM algorithm [45]. The differential gene expression was analyzed by the multifactor generalized linear model (GLM) approach in edgeR with replicate number added as a factor to the GLM to mitigate for a batch effect. The filtered genes with a *p*-value under 0.05 were considered as differential expressed genes. Gene ontology (GO) and Kyoto Encyclopedia of Genes and Genomes (KEGG) pathway were performed by g:Profiler for computing multiple hypothesis testing corrections (g:scs < 0.05) [46]. The ReViGO was used to summarize and visualize the list of significantly enriched GO terms based on semantic similarities (allowed similarity: 0.5) [47]. The RNA-seq data used in this study have been deposited in the Gene Expression Omnibus (GEO: http:/www.ncbi.nlm.nih.gov/geo/) and assigned the identifier accession GSE157230 and GSE158133.

Detecting oscillation genes

The RNA-seq dataset for UR detection (synchronized RNA-seq dataset) was analyzed by bioinformatics tools (described above). The MetaCycle R package which incorporates ARSER, JTK CYCLE and Lomb-Scargle [27] was used to detect rhythmic genes from Synchronized RNA-seq data. The ultradian rhythms were detected with parameters: minper 2 h and maxper 5 h. The genes with cut-off (*p*-value < 0.05) based on meta2d results were defined as UR oscillating genes.

Clustering for differential expressed genes in *eur1-11*

The expression values of DEGs were analyzed by the tri-cluster system, TimesVector [48] for the relationship between time series and pattern of DEGs.

ABA seed germination and primary root growth assay

The seeds were sown on ½ B5 medium (Duchefa, The Netherlands) containing 2% (w/v) sucrose and 0.8% agar, incubated under a 16 h light/8 h dark cycle with a light intensity of ~100 μmol m^{-2} s^{-1} light at 22°C in the environmentally controlled growth room. For the seed germination assay, 30 seeds were sown on ½ B5 medium containing different concentration of ABA. The plates were incubated under a 16 h light/8 h dark cycle with a light intensity of ~100 μmol m^{-2} s^{-1} light at 22°C in the environmentally controlled growth room for 8 days to examine the seed germination ratio. For the primary root growth assay, 6 day-old seedlings were transferred to vertical plates of ½ B5 medium containing different

concentrations of ABA and grown for an additional 4 days. The plates were then scanned by HP Scanjet 8300 and primary root length was measured by ImageJ program.

EMS Mutagenesis and Screening assay for the UR regulators

Approximately 20,000 seeds (M1) of Col-0/*ORE1::LUC* line were mutagenized by treatment with 0.3% or 0.33% ethyl methanesultonate (EMS) solution for 8 hours. M2 seeds were obtained by self-fertilization of the M1 plants. M2 seeds were sown on half strength B5 medium (Duchefa, The Netherlands) containing 1% sucrose and 0.8% agar (pH 5.7). The plates were placed under 16h light/8h dark (LD) with ~100 μmol m^{-2} s^{-1} light at 22°C in the environmentally controlled growth room until 2 weeks-old. The 1^{st} or 2^{nd} leaves were excised by forceps at the petiole base and transferred to 96-well microplates containing 500μM luciferin (SYNCHEM, Felsberg/Altenburg, Germany). Luminescence images were acquired every 30 min for at least 3 days under continuous white light conditions at 22^{o}C by CCD camera. 16 experimental runs were done to check UR patterns in excised leaves from ~16,000 M2 plants. 175 M2 plants whose excised leaves not showing the UR were selected as candidates for the UR regulators. Because the UR was fragile and sensitive with aging, we only selected plants completely removing the UR with maintaining green after leaf excision across UR measuring time as Col-0/*ORE1::LUC* parent. These selected plants were moved to soil and grew for M3 seeds. We after that re-checked UR pattern in excised leaves with at least 8 M3 plants of each selected mutant lines. 28 mutant lines in M3 were confirmed with UR disappearance in excised leaves. Among 28 lines, we finally found 4 homozygous lines not showing the UR in excised leaves and selected those lines as candidates of the UR regulators for further investigation.

Genomic DNA Library Preparation for Whole Genome Sequencing (WGS)

For WGS, pools of genomic DNA were prepared from 20-25 seedlings of 14 day-old plate-grown Col/*ORE1::LUC* as control and *eur1-11*, *eur1-13* backcrossed with Col/*ORE1::LUC* F2 not showing the UR in excised leaves. After grinding samples in the liquid nitrogen, genomic DNA was extracted by CTAB (cetyltrimethyl ammonium bromide) extraction buffer containing 100 mM Tris-HCl (pH 8.0), 20 mM EDTA (pH 8.0), 1.4 M NaCl, 2% (W/V) CTAB and 1% PVP 40, 000 (polyvinyl pyrrolidone) and mixture of phenol/chloroform/isoamyl alcohol (25:24:1) (Thermo Scientific). Contaminating RNA was removed by adding 2.5μl of RNAse A (10 mg/ml) (Roche) in every 500μl of CTAB extraction buffer. Genomic DNA products finally were purified by QIAGEN Dneasy Plant Mini Kit.

Whole genome sequence and SNP detection in EMS mutants

The DNA library construction from EMS mutants was prepared using Truseq Nano DNA Prep Kit (Illumina, San Diego, CA, USA). The quality was verified by Agilent 2100 Bioanalyzer (Agilent, Santa Clara, CA, USA), then the passed libraries were loaded onto NovaSeq 6000 Sequencing system (Illumina, San Diego, CA, USA) by DNALink, South Korea (https://www.dnalink.com), as instructed in the manufacturer's protocols. The reads were quality checked and filtered by fastp [49]. The clean reads were aligned to the reference genome of TAIR10 and genetic variants were called according to SIMPLE pipeline [50].

Microscopic assay

To confirm EAR1 protein levels in petiole region, the 1st or 2nd rosette leaves were excised from plate grown 14-day-old plants. The leaf explants were cultured on half strength B5 medium without sucrose and incubated under continuous light conditions with ~20 μmol $m^{-2}s^{-1}$ white light at 22^{o}C. For confocal laser scanning microscopy, samples at indicated time were observed using a Zeiss LSM 7 DUO system (Carl Zeiss), with a 20 x objective. Wavelengths used to visualize GFP and autofluorescence of chloroplasts were 500-540 and 600-640 nm, respectively. Tiled images were taken with ZEN software (Carl Zeiss) and processed with Adobe Photoshop.

Declarations

Acknowledgements: We thank Robertson McClung, Steve Kay, Philip Benfey and NASC for sharing research materials. We also thank KH Suh, HH Cho, SH Jung and GY Seo for technical assistance.

Funding: Institute for Basic Science (IBS) grant IBS-R013-D1 (HGN, SH).

Author contributions:

Conceptualization: QTV, KS, HGN, SH

Methodology: QTV, KS, SH

Formal analysis: KS, SH

Investigation: QTV, SP, SH

Supervision: HGN, SH

Writing – original draft: QTV, KS, SH

Writing – review & editing: LX, HGN, SH

Competing interests: Authors declare that they have no competing interests.

Data and materials availability: All data are available in the main text or the supplementary information.

References

1 McClung, C. R. The genetics of plant clocks. *Advances in genetics* **74**, 105-139 (2011).

2 Laje, R., Agostino, P. V. & Golombek, D. A. The times of our lives: interaction among different biological periodicities. *Frontiers in integrative neuroscience* **12**, 10 (2018).

3 Prendergast, B. J. & Zucker, I. Ultradian rhythms in mammalian physiology and behavior. *Current opinion in neurobiology* **40**, 150-154 (2016).

4 Aulehla, A. & Pourquié, O. Oscillating signaling pathways during embryonic development. *Current opinion in cell biology* **20**, 632-637 (2008).

5 Moreno-Risueno, M. A. *et al.* Oscillating gene expression determines competence for periodic Arabidopsis root branching. *Science* **329**, 1306-1311 (2010).

6 Isomura, A. & Kageyama, R. Ultradian oscillations and pulses: coordinating cellular responses and cell fate decisions. *Development* **141**, 3627-3636 (2014).

7 Zhu, B. *et al.* A cell-autonomous mammalian 12 hr clock coordinates metabolic and stress rhythms. *Cell metabolism* **25**, 1305-1319. e1309 (2017).

8 McAinsh, M. R., Webb, A. A., Taylor, J. E. & Hetherington, A. M. Stimulus-induced oscillations in guard cell cytosolic free calcium. *The Plant Cell* **7**, 1207-1219 (1995).

9 Staxén, I. *et al.* Abscisic acid induces oscillations in guard-cell cytosolic free calcium that involve phosphoinositide-specific phospholipase C. *Proceedings of the National Academy of Sciences* **96**, 1779-1784 (1999).

10 Allen, G. J. *et al.* Alteration of stimulus-specific guard cell calcium oscillations and stomatal closing in Arabidopsis det3 mutant. *Science* **289**, 2338-2342 (2000).

11 Goh, G. H., Maloney, S. K., Mark, P. J. & Blache, D. Episodic ultradian events—ultradian rhythms. *Biology* **8**, 15 (2019).

12 Wollnik, F. Physiology and regulation of biological rhythms in laboratory animals: an overview. *Laboratory animals* **23**, 107-125 (1989).

13 Stoick-Cooper, C. L., Moon, R. T. & Weidinger, G. Advances in signaling in vertebrate regeneration as a prelude to regenerative medicine. *Genes & development* **21**, 1292-1315 (2007).

14 Ikeuchi, M. *et al.* Molecular mechanisms of plant regeneration. *Annual review of plant biology* **70**, 377-406 (2019).

15 Ikeuchi, M., Ogawa, Y., Iwase, A. & Sugimoto, K. Plant regeneration: cellular origins and molecular mechanisms. *Development* **143**, 1442-1451 (2016).

16 Lup, S. D., Tian, X., Xu, J. & Pérez-Pérez, J. M. Wound signaling of regenerative cell reprogramming. *Plant Science* **250**, 178-187 (2016).

17 Xu, L. & Huang, H. Genetic and epigenetic controls of plant regeneration. *Current topics in developmental biology* **108**, 1-33 (2014).

18 Chen, X. *et al.* A simple method suitable to study de novo root organogenesis. *Frontiers in Plant Science* **5**, 208 (2014).

19 Xu, L. De novo root regeneration from leaf explants: wounding, auxin, and cell fate transition. *Current opinion in plant biology* **41**, 39-45 (2018).

20 Jing, T., Ardiansyah, R., Xu, Q., Xing, Q. & Müller-Xing, R. Reprogramming of Cell Fate During Root Regeneration by Transcriptional and Epigenetic Networks. *Frontiers in Plant Science* **11**, 317 (2020).

21 Kim, H. *et al.* Circadian control of ORE1 by PRR9 positively regulates leaf senescence in Arabidopsis. *Proceedings of the National Academy of Sciences* **115**, 8448-8453 (2018).

22 Kim, H., Kim, Y., Yeom, M., Lim, J. & Nam, H. G. Age-associated circadian period changes in Arabidopsis leaves. *Journal of experimental botany* **67**, 2665-2673 (2016).

23 Leise, T. L. Wavelet analysis of circadian and ultradian behavioral rhythms. *Journal of circadian rhythms* **11**, 5 (2013).

24 Chen, L. *et al.* YUCCA-mediated auxin biogenesis is required for cell fate transition occurring during de novo root organogenesis in Arabidopsis. *Journal of experimental botany* **67**, 4273-4284 (2016).

25 Bustillo-Avendaño, E. *et al.* Regulation of hormonal control, cell reprogramming, and patterning during de novo root organogenesis. *Plant physiology* **176**, 1709-1727 (2018).

26 Nishimura, T. *et al.* Yucasin is a potent inhibitor of YUCCA, a key enzyme in auxin biosynthesis. *The Plant Journal* **77**, 352-366 (2014).

27 Wu, G., Anafi, R. C., Hughes, M. E., Kornacker, K. & Hogenesch, J. B. MetaCycle: an integrated R package to evaluate periodicity in large scale data. *Bioinformatics* **32**, 3351-3353 (2016).

28 Pan, J. *et al.* Control of de novo root regeneration efficiency by developmental status of Arabidopsis leaf explants. *Journal of Genetics and Genomics* **46**, 133-140 (2019).

29 Wang, K. *et al.* EAR1 negatively regulates ABA signaling by enhancing 2C protein phosphatase activity. *The Plant Cell* **30**, 815-834 (2018).

30 Palmeirim, I., Henrique, D., Ish-Horowicz, D. & Pourquié, O. Avian hairy gene expression identifies a molecular clock linked to vertebrate segmentation and somitogenesis. *Cell* **91**, 639-648 (1997).

31 Pourquié, O. The segmentation clock: converting embryonic time into spatial pattern. *Science* **301**, 328-330 (2003).

32 Gala, H. P. *et al.* A single cell view of the transcriptome during lateral root initiation in Arabidopsis thaliana. *bioRxiv* (2020).

33 Ye, B.-B. *et al.* AP2/ERF transcription factors integrate age and wound signals for root regeneration. *The Plant Cell* **32**, 226-241 (2020).

34 Li, H., Yao, L., Sun, L. & Zhu, Z. ETHYLENE INSENSITIVE 3 suppresses plant de novo root regeneration from leaf explants and mediates age-regulated regeneration decline. *Development* **147** (2020).

35 Lakehal, A. & Bellini, C. Control of adventitious root formation: insights into synergistic and antagonistic hormonal interactions. *Physiologia plantarum* **165**, 90-100 (2019).

36 Salomé, P. A. & McClung, C. R. PSEUDO-RESPONSE REGULATOR 7 and 9 are partially redundant genes essential for the temperature responsiveness of the Arabidopsis circadian clock. *The Plant Cell* **17**, 791-803 (2005).

37 Millar, A. J., Short, S. R., Chua, N. H. & Kay, S. A. A novel circadian phenotype based on firefly luciferase expression in transgenic plants. *The Plant Cell* **4**, 1075-1087 (1992).

38 Kim, B. C., Soh, M. S., Hong, S. H., Furuya, M. & Nam, H. G. Photomorphogenic development of the Arabidopsisshy2–1D mutation and its interaction with phytochromes in darkness. *The Plant Journal* **15**, 61-68 (1998).

39 Ruegger, M. *et al.* The TIR1 protein of Arabidopsis functions in auxin response and is related to human SKP2 and yeast Grr1p. *Genes & development* **12**, 198-207 (1998).

40 Schultz, T. F., Kiyosue, T., Yanovsky, M., Wada, M. & Kay, S. A. A role for LKP2 in the circadian clock of Arabidopsis. *The Plant Cell* **13**, 2659-2670 (2001).

41 Rösch, A. & Schmidbauer, H. WaveletComp 1.1: A guided tour through the R package. *URL: http://www. hsstat. com/projects/WaveletComp/WaveletComp_guided_tour. pdf* (2016).

42 Andrews, S. (Babraham Bioinformatics, Babraham Institute, Cambridge, United Kingdom, 2010).

43 Dobin, A. *et al.* STAR: ultrafast universal RNA-seq aligner. *Bioinformatics* **29**, 15-21 (2013).

44 Anders, S., Pyl, P. T. & Huber, W. HTSeq—a Python framework to work with high-throughput sequencing data. *Bioinformatics* **31**, 166-169 (2015).

45 Robinson, M. D., McCarthy, D. J. & Smyth, G. K. edgeR: a Bioconductor package for differential expression analysis of digital gene expression data. *Bioinformatics* **26**, 139-140 (2010).

46 Reimand, J., Kull, M., Peterson, H., Hansen, J. & Vilo, J. g: Profiler—a web-based toolset for functional profiling of gene lists from large-scale experiments. *Nucleic acids research* **35**, W193-W200 (2007).

47 Supek, F., Bošnjak, M., Škunca, N. & Šmuc, T. REVIGO summarizes and visualizes long lists of gene ontology terms. *PloS one* **6**, e21800 (2011).

48 Jung, I. *et al.* TimesVector: a vectorized clustering approach to the analysis of time series transcriptome data from multiple phenotypes. *Bioinformatics* **33**, 3827-3835 (2017).

49 Chen, S., Zhou, Y., Chen, Y. & Gu, J. fastp: an ultra-fast all-in-one FASTQ preprocessor. *Bioinformatics* **34**, i884-i890 (2018).

50 Wachsman, G., Modliszewski, J. L., Valdes, M. & Benfey, P. N. A SIMPLE pipeline for mapping point mutations. *Plant physiology* **174**, 1307-1313 (2017).

Figures

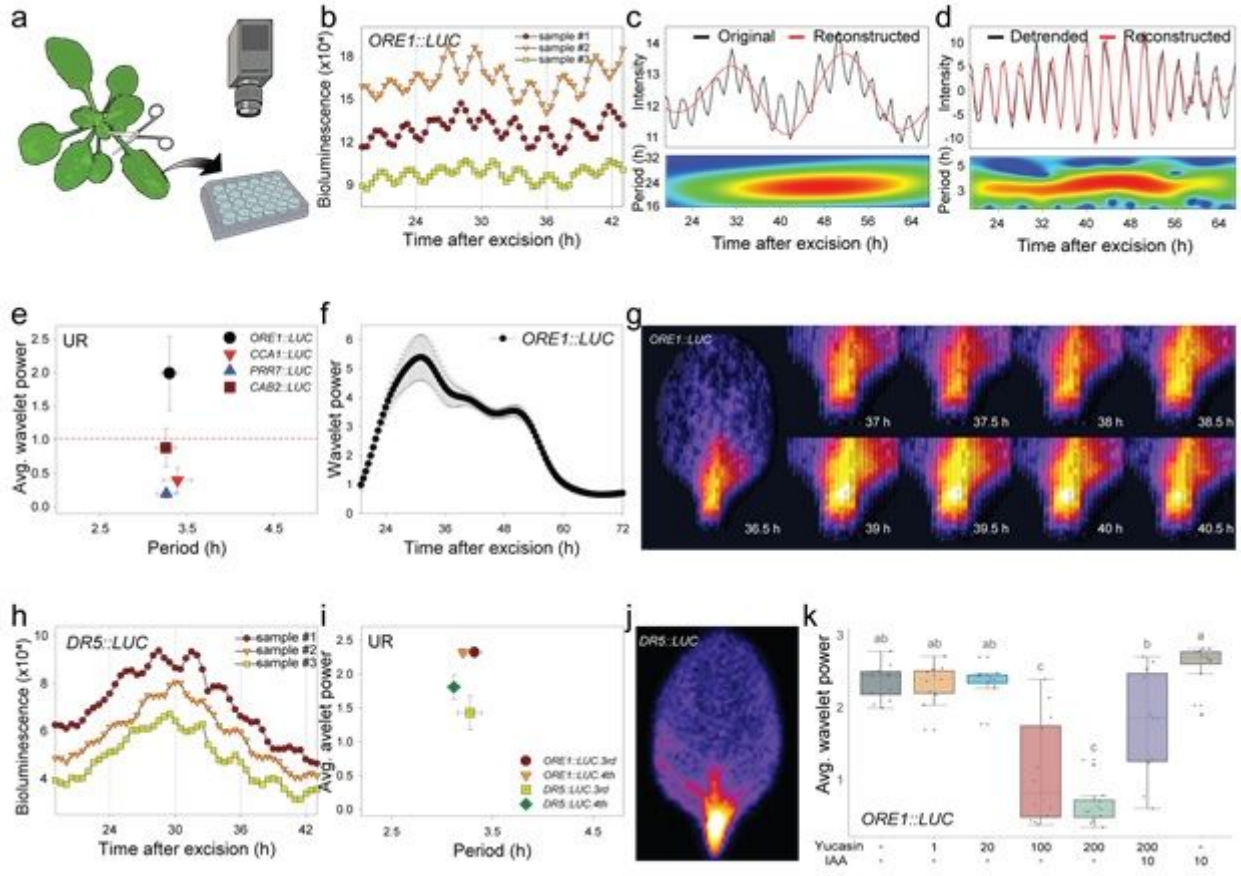

Figure 1

An excision-triggered ultradian rhythm is mediated by auxin in Arabidopsis leaves. a, Experimental setup used to measure luminescence in the leaves of transgenic Arabidopsis plants expressing ORE1::LUC. b, ORE1 promoter activity in Arabidopsis leaves at the indicated time points. The graph shows three representative samples. At least three different experiments were performed with similar results. c,d, Wavelet analysis-based decomposition of ORE1 promoter activity showing (c) circadian rhythm (CR) and

(d) ultradian rhythm (UR). Black and red lines (upper panels) represent luminescence intensity and reconstructed rhythm, respectively. Wavelet spectrum plots (lower panels) indicate period range and wavelet power through the indicated time period. Red and blue indicate higher and lower wavelet powers, respectively. e, Average wavelet powers and periods of UR in the activities of ORE1, CCA1, PRR7 and CAB2 promoters, as quantified by wavelet analysis. Data are means ± s.e.m. (n = 24 leaves). Red line indicates the UR threshold. f, Instantaneous UR wavelet power of ORE1 promoter activity in ORE1::LUC leaves. The wavelet power for UR shows the distribution of UR through the indicated time period. Data are means ± s.e.m. (n = 24 leaves). g, Time-series analysis of ORE1::LUC expression in the petiole region after leaf excision. h, DR5::LUC activity in excised Arabidopsis leaves at the indicated time points. The graph shows three representative samples. i, Average wavelet powers and periods of UR in ORE1 and DR5 promoter activities in excised leaves, as determined by wavelet analysis. Data are means ± s.e.m. (n = 12 leaves). j, Image showing DR5::LUC luminescence in an excised leaf. k, Average wavelet powers of UR in excised leaves expressing ORE1::LUC treated exogenously with yucasin or indole-3-acetic acid (IAA) (n = 24 leaves). Centre line: median; bounds of box: 25th and 75th percentiles; whiskers: 1.5 × IQR from 25th and 75th percentiles. Statistical significance was determined by one-way analysis of variance (ANOVA) with Tukey's post hoc test. Data points with different letters indicate statistically significant differences between groups ($P < 0.01$).

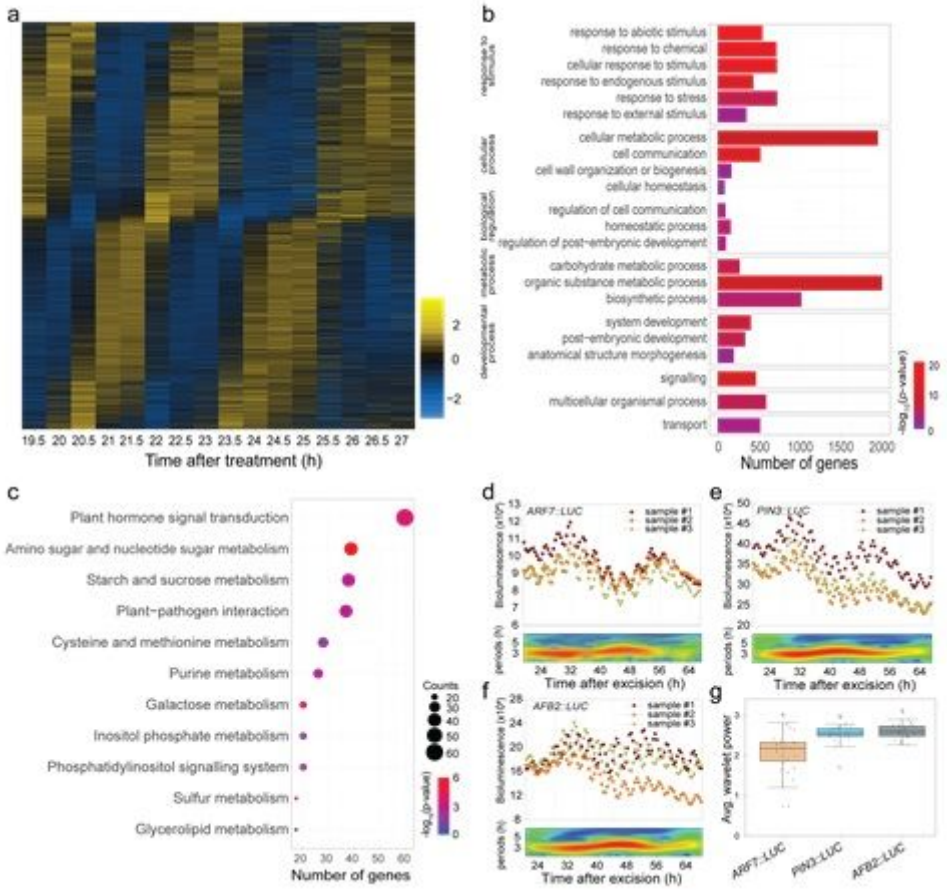

Figure 2

Transcriptomic and functional analysis of the excision UR genes. a, Heat map showing the expression levels of genes oscillating over time. Yellow and blue indicate higher and lower relative expression, respectively. b, Gene ontology enrichment analysis of the excision UR genes. Bars represent numbers of genes and color represents the p value. c, KEGG enrichment analysis of the excision UR genes. Dot size indicates the number of genes, and dot colour represents the P-value. d,f, Analysis of ARF7, PIN3 and AFB2 promoter activities using the LUC reporter. Graphs show data from three representative samples. The graphs (upper panels) show measurements from three representative samples (n = 24) and the wavelet spectrum plots (lower panels) show merged wavelet power plots of all samples with low transparency. g, Average wavelet powers of the excision UR of ARF7, PIN3 and AFB2 (n = 24 leaves). Centre line: median; bounds of box: 25th and 75th percentiles; whiskers: 1.5 × IQR from 25th and 75th percentiles. Statistical significance was determined by one-way analysis of variance (ANOVA) with Tukey's post hoc test. Data points with different letters indicate statistically significant differences between groups ($P < 0.01$).

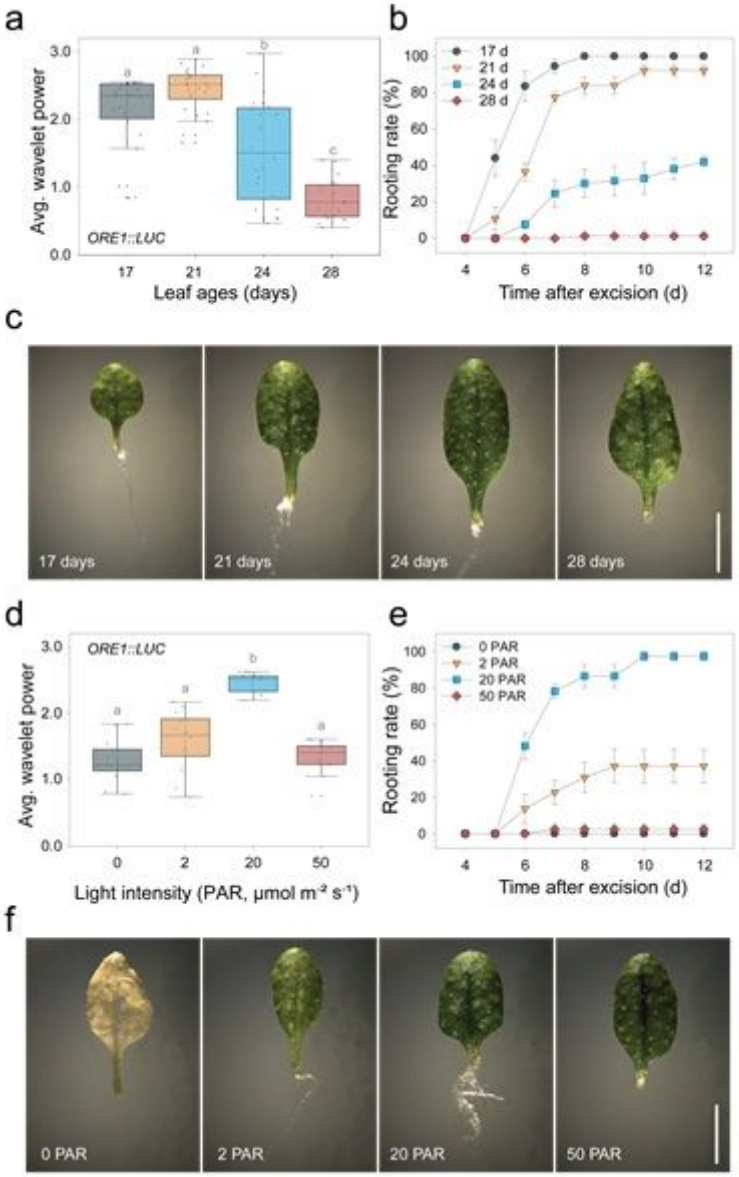

Figure 3

Positive correlation between the excision UR and de novo root regeneration (DNRR). a, Average wavelet powers of the excision UR in wild-type leaves excised from plants of different ages (n = 24 leaves). b, Rooting rates of wild-type leaves of different ages. Data are means ± s.e.m. from three independent replicates. c, Images showing root regeneration 10 days after excision in wild-type leaves of different ages. Scale bar: 5 mm. d, Average wavelet powers of the excision UR in wild-type leaves exposed to different light intensities (n = 24 leaves). In a,d, centre line: median; bounds of box: 25th and 75th percentiles; whiskers: 1.5 × IQR from 25th and 75th percentiles. Statistical significance was determined by one-way analysis of variance (ANOVA) with Tukey's post hoc test. Data points with different letters indicate statistically significant differences between groups (P < 0.01). e, Rooting rates in wild-type leaves exposed to different light intensities. Data are means ± s.e.m. from three independent replicates. f, Images showing root regeneration from wild-type leaves under different light intensities.

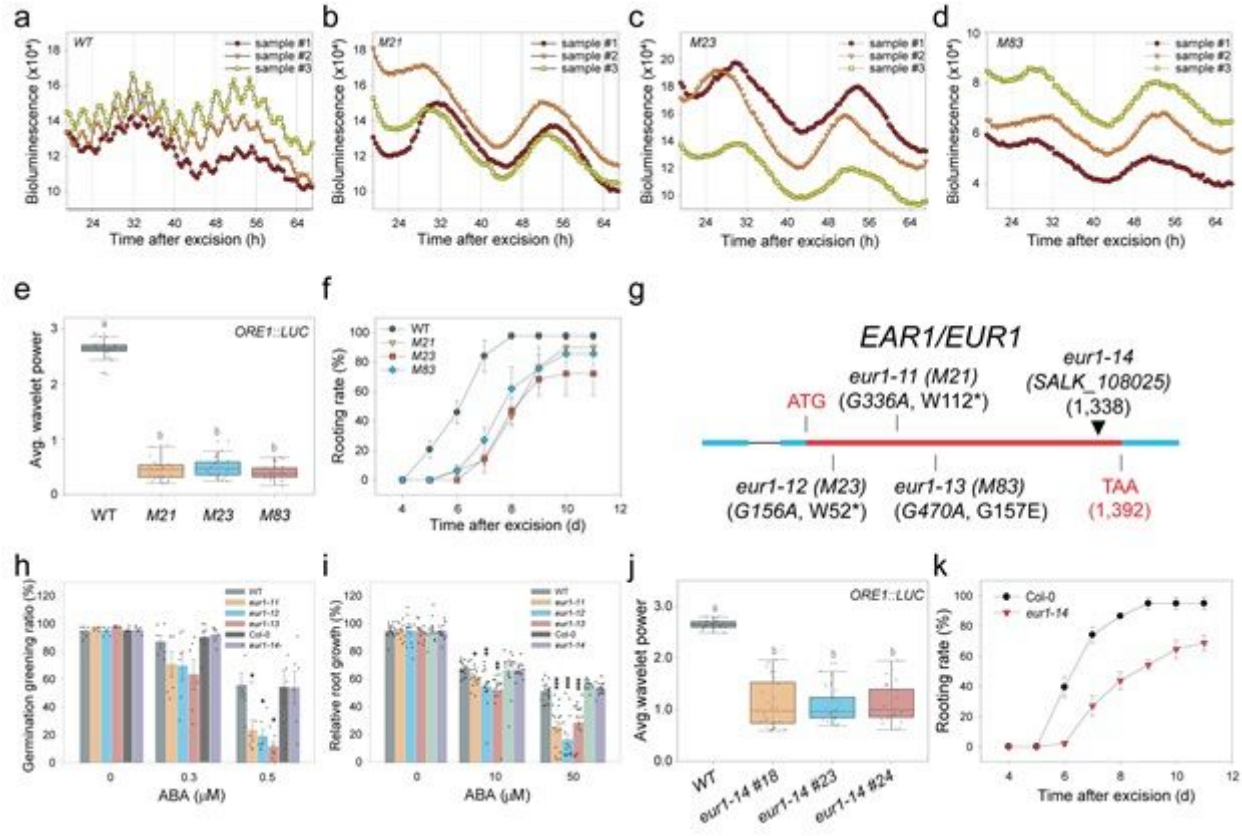

Figure 4

EAR1/EUR1, an abscisic acid signaling component, regulates the excision UR to optimize DNRR. a-d, ORE1 promoter activity in ORE1::LUC transgenic plants and EMS-mutagenized mutant candidates. (a) wild type (WT); (b) M21; (c) M23; (d) M83. Graphs show data from three representative samples. e, Average wavelet powers of the excision UR in WT plants and mutant candidates (n = 24 leaves). f, Rooting rates of WT plants and mutant candidates. Data are means ± s.e.m. from three independent replicates. g, Schematic representation of the mutation sites in eur1-11 (M21), eur1-12 (M23), eur1-13 (M83) and eur1-14 (SALK_108025). h,i, Effects of treatment of wild type, eur1-11, eur1-12, eur1-13, and eur1-14 plants with exogenous ABA on germination greening ratio (n = 6) (h) and relative root growth (i) (n = 13 seedlings). Two-tailed t-test was used between wild type and eur1 mutants (*p £ 0.05, ** p £ 0.01,

*** p £ 0.001) j, Average wavelet powers of the excision UR of wild type, eur1-14 #18, eur1-14 #23 and eur1-14 #24 (n = 24 leaves). k, Rooting rates of Col-0 and eur1-14. Data are means ± s.e.m. from three independent replicates.

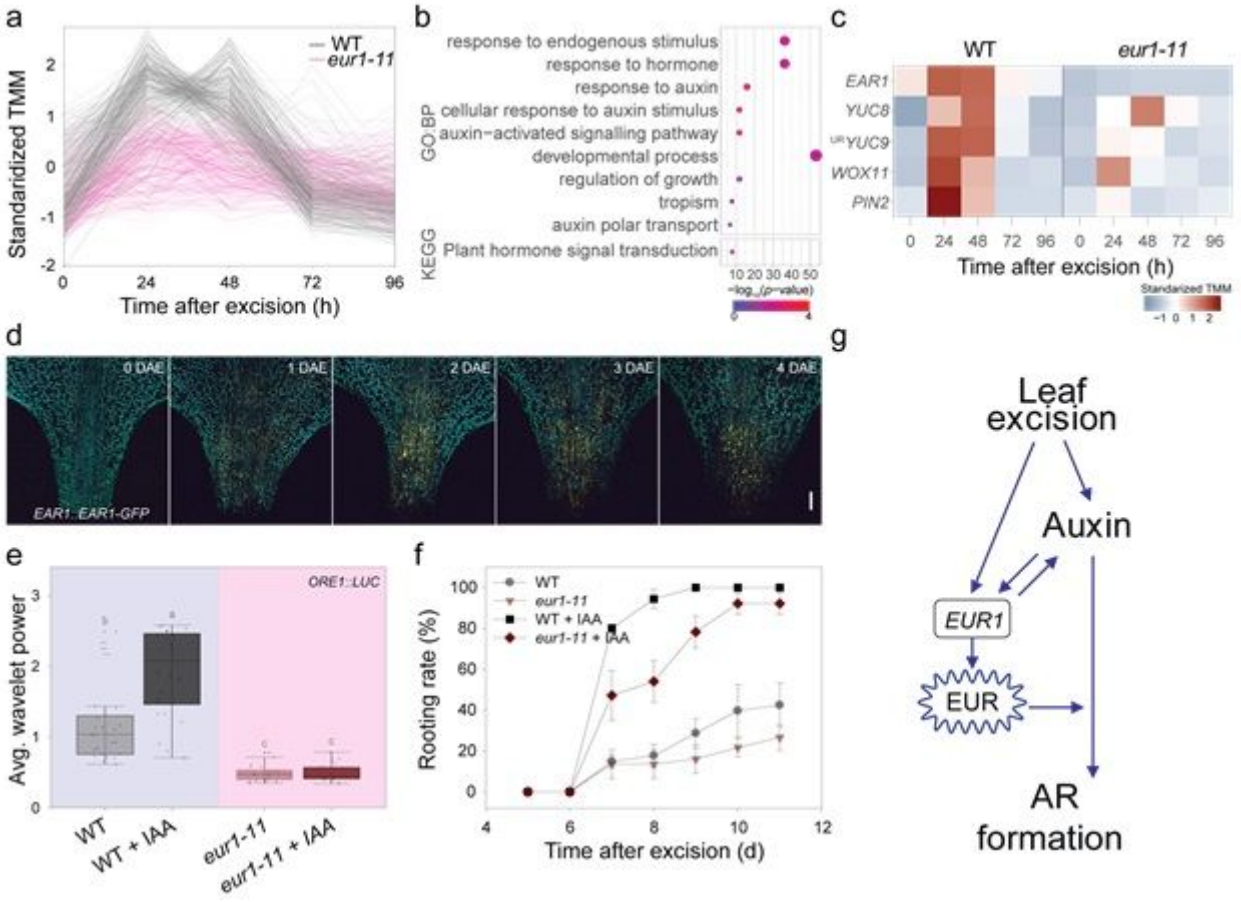

Figure 5

EAR1/EUR1 mediates generation of the auxin-induced excision UR to promote DNRR. a, Expression patterns of cluster 2 genes, which include EAR1/EUR1. b, Gene ontology (GO) enrichment analysis of genes in cluster 2. Dot size indicates the number of genes, and dot colour indicates the P-value. c, Heat map of DNRR-associated genes belonging to cluster 2. Expression values from RNA-seq were standardized to allow comparison. d, Tiled confocal images of the petiole region of COM-9 (EAR1::EAR1-GFP) leaves. Yellow indicates EAR1-GFP fluorescence; blue indicates chlorophyll autofluorescence. Two independent lines were analysed with similar results. Scale bar: 0.2 mm. e,f, Effect of IAA treatment on average wavelet powers of the excision UR (e) (n = 24 leaves) and rooting rates of wild-type and eur1 leaves excised from 24-day-old plants (f). Centre line: median; bounds of box: 25th and 75th percentiles; whiskers: 1.5 × IQR from 25th and 75th percentiles. Statistical significance was determined by one-way analysis of variance (ANOVA) with Tukey's post hoc test. Data points with different letters indicate statistically significant differences between groups (P < 0.01). In f, data are means ± s.e.m. from three independent replicates. g, Schematic showing EAR1/EUR1-mediated excision UR generation and DNRR in excised leaves.

Supplementary Files

This is a list of supplementary files associated with this preprint. Click to download.

- QuyetalNaturePSTable1.xlsx
- QuyetalNaturePSTable2.xlsx
- QuyetalNaturePSTable3.xlsx
- QuyetalNaturePSTable4.xlsx
- QuyetalNaturePSTable5.xlsx
- QuyetalNaturePSMovie1.mp4
- SupplementaryFigure1.jpg
- SupplementaryFigure2.jpg
- SupplementaryFigure3.jpg
- SupplementaryFigure4.jpg
- SupplementaryFigure5.jpg
- SupplementaryFigure6.jpg
- SupplementaryFigure7.jpg